Available online at www.elixirpublishers.com (Elixir International Journal)

Computational Chemistry

Elixir Comp. Chem. 44 (2012) 7425-7429

ISSN: 2229-712X

Scaled quantum chemical studies of the structure, vibrational spectra and first-order hyperpolarizability of 2-amino-4-pyrimidinol

V.Balakrishnan[1,*] and P.M.Andavan[2]

[1]Department of Physics, Dravidian University, Kuppam - 517 425,India.

[2]Department of Physics, Government Arts College (Autonomous), Coimbatore - 641 018,India.

ARTICLE INFO

Article history:

Received: 16 September 2011;

Received in revised form:

13 March 2012;

Accepted: 22 March 2012;

Keywords

Vibrational analysis,

Infrared and Raman spectra,

DFTcalculations.

ABSTRACT

FT-IR and FT-Raman spectra of 2-amino-4-pyrimidinol (2A4P) have been recorded. The spectra were interpreted with the aid of normal coordinate analysis following full structure optimizations and force field calculations based on density functional theory (DFT) using standard B3LYP/6-311+G** method. Normal coordinate calculations were performed with the DFT force field corrected by a recommended set of scaling factors yielding fairly good agreement between observed and calculated frequencies. Further, density functional theory (DFT) combined with quantum chemical calculations to determine the first-order hyperpolarizability.

Introduction

Modern vibrational spectrometry has proven to be an exceptionally powerful technique for solving many chemical problems. It has been extensively employed both in the study of chemical kinetics and chemical analysis. The problem of signal assignment however, as well as understanding the relationship between the observed spectral features and molecular structure, and reactivity can be difficult. Even identification of fundamental vibrational frequencies often generates controversy. However, for a proper understanding of IR and Raman, a reliable assignment of all vibrational band is essential. Recently, computational methods based on density functional theory (DFT) are becoming widely used and these methods predict relatively accurate molecular structure and vibrational spectra with moderate computational effort. In particular, for polyatomic molecules the DFT methods lead to the prediction of more accurate molecular structure and vibrational frequencies than the conventional ab initio restricted Hartree-Fock (RHF) and Moller-plesset second order perturbation theory (MP2) calculations. Among the DFT calculation, Becke's [1] three parameter hybrid functional combined with the Lee–Yang–Parr [2] correlation functional (B3LYP) is the best in predicting results for molecular geometry and vibrational wave numbers for moderately larger molecules. To gain a better understanding of the performance and limits of DFT methods as a general approach to the vibrational problems of organic molecules, we calculated harmonic frequencies of 2-amino-4-pyrimidinol (2A4P) by DFT method, and compared these results with observed fundamental vibrational frequencies. The symmetry analysis for the vibrational modes of 2A4P is presented in some details in order to describe the basis for the assignments. By combining the results of the GAUSSVIEW program [3] with symmetry considerations, vibrational frequency assignments were made with a high degree of confidence. There is always some ambiguity in defining internal coordination. However, the defined coordinate form complete set and matches quite well with motions observed using the GAUSSVIEW program. The aim of this work is to check the performance of B3LYP density functional force field for simulation of IR and Raman spectra of the title compound with the use of standard 6-31G* and 6-311+G** basis sets (referred to as small and large basis set, respectively). The simulated and observed spectra were analysed in detail. Unambiguous vibrational assignment of all the fundamentals was made using the total energy distribution (TED). Further, density functional theory (DFT) combined with quantum chemical calculations to determine the first-order hyperpolarizability.

Experimental details

The fine samples of 2A4P were obtained from Lancaster Chemical Company, UK, and used as such for the spectral measurements. The room temperature Fourier transform infrared spectra of the title compounds were measured in the region 4000-400 cm^{-1} at a resolution of ±1 cm^{-1}, using BRUKER IFS 66V vacuum Fourier transform spectrometer, equipped with an MCT detector, a KBr beam splitter and globar source. The FT-Raman spectra were recorded on the same instrument with FRA 106 Raman accessories in the region 3500-100 cm^{-1}. Nd:YAG laser operating at 200 mw power with 1064 nm excitation was used as source.

Computational details

Quantum chemical calculations for 2A4P were performed with the GAUSSIAN 03W program using the Becke-3–Lee–Yang–Parr [1,2] (B3LYP) functionals supplemented with the 6-311+G^{**} basis sets (referred large basis sets), for the Cartesian representation of the theoretical force constants have been computed at the fully optimized geometry by assuming C_s point group symmetry. Scaling of the force field was performed according to the SQM procedure using selective (multiple) scaling in the natural internal coordinate representation. Transformations of the force field and the subsequent normal coordinate analysis including the least squares refinement of the scaling factors, calculation of total energy distribution (TED) and IR and Raman intensities were done on a PC with the

Tele:

E-mail addresses: photonic_ss@rediffmail.com

MOLVIB program (Version V7.0-G77) written by Sundius [4]. The TED elements provide a measure of each internal coordinate's contribution to the normal coordinate. For the plots of simulated IR and Raman spectra, pure Lorentzian band shapes were used with a band width (FWHM) of 10 cm^{-1}.

Prediction of Raman intensities

The Raman activities (Si) calculated with the GAUSSIAN 03W program and adjusted during the scaling procedure with MOLVIB were subsequently converted to relative Raman intensities (Ii) using the following relationship derived from the basic theory of Raman scattering [5-7].

$$I_i = \frac{f(v_o - v_i)^4 S_i}{v_i[1-\exp(-hcv_i / KT)} \text{ ----------(1)}$$

Where υ_0 is the exciting frequency (in cm^{-1}), υ_i is the vibrational wavenumber of the i^{th} normal mode; h, c and k are fundamental constants, and f is a suitably chosen common normalization factor for all peak intensities.

Essentials of nonlinear optics related to β

The nonlinear response of an isolated molecule in an electric field $E_i(\omega)$ can be represented as a Taylor expansion of the total dipole moment μ_t induced by the field:

$$\mu_t = \mu_0 + \alpha_{ij}E_i + \beta_{ijk}E_iE_j + ...$$

Where α is linear polarizability, μ_0 the permanent dipole moment and β_{ijk} are the first-order hyperpolarizability tensor components.

The components of first-order hyperpolarizability can be determined using the relation

$$\beta_i = \beta_{iii} + \frac{1}{3}\sum_{i \neq j}(\beta_{ijj} + \beta_{jij} + \beta_{jji})$$

Using the x, y and z components the magnitude of the total static dipole moment (μ), isotropic polarizability (α_0), first-order hyperpolarizability (β_{total}) tensor, can be calculated by the following equations:

$$\mu_1^0 = (\mu_x^2 + \mu_y^2 + \mu_z^2)^{1/2}$$

$$\beta_{tot} = (\beta_x^2 + \beta_y^2 + \beta_z^2)^{1/2}$$

The complete equation for calculating the first-order hyperpolarizability from GAUSSIAN 03W output is given as follows:

$$\beta_{tot} = [(\beta_{xxx} + \beta_{xyy} + \beta_{xzz})^2 + (\beta_{yyy} + \beta_{yzz} + \beta_{yxx})^2 + (\beta_{zzz} + \beta_{zxx} + \beta_{zyy})^2]$$

The β components of GAUSSIAN 03W output are reported in atomic units, the calculated values have to be converted into electrostatic units (1 a.u= 8.3693 $x10^{-33}$ esu).

Before calculating the hyperpolarizability for the investigated compound, the optimization has been carried out in the UHF (unrestricted open-shell Hartree-Fock) level. Molecular geometries were fully optimized by Berny's optimization algorithm using redundant internal coordinates. All optimized structures were confirmed to be minimum energy conformations. An optimization is complete when it has converged. i.e., when it has reached a minimum on the potential energy surface, thereby predicting the equilibrium structures of the molecules. This criterion is very important in geometry optimization. The inclusion of d polarization and double zeta function in the split valence basis set is expected to produce a marked improvement in the calculated geometry [1]. At the optimized structure, no imaginary frequency modes were obtained proving that a true minimum on the potential energy surface was found. The electric dipole moment and dispersion free first-order hyperpolarizibility were calculated using finite field method. The finite field method offers a straight forward approach to the calculation of hyperpolarizabilities [8]. All the calculations were carried out at the DFT level using the three-parameter hybrid density functional B3LYP and a 3-21 G (d, p) basis set.

Results and discussion

Molecular geometry

The optimized molecular structure of 2A4P was shown in Fig. 1. The global minimum energy obtained by the DFT structure optimization was presented in Table 1. The optimized geometrical parameters obtained by the large basis set calculation were presented in Table 2.

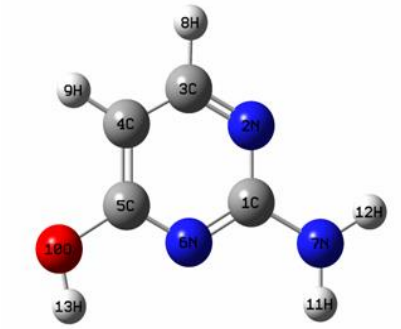

Fig. 1. The optimized molecular structure of 2A4P

Detailed description of vibrational modes can be given by means of normal coordinate analysis (NCA). For this purpose, the full set of 44 standard internal coordinates containing 11 redundancies were defined as given in Table 3. From these, a non-redundant set of local symmetry coordinates were constructed by suitable linear combinations of internal coordinates following the recommendations of Fogarasi et. al [9] are summarized in Table 4. The theoretically calculated DFT force fields were transformed in this later set of vibrational coordinates and used in all subsequent calculations.

Table 1. Total energies of 2A4P, calculated at DFT (B3LYP)/6-31G* and (B3LYP)/6-311+G level**

Method	Energies (Hartrees)
6-31G*	-394.77438721
6-311+G**	-394.92952395

Analysis of vibrational spectra

The 33 normal modes of 2A4P are distributed among the symmetry species as Γ_{3N-6}= 23 A' (in-plane) + 10 A″ (out-of-plane), and in agreement with C_s symmetry. All the vibrations were active both in Raman scattering and infrared absorption. In the Raman spectrum the in-plane vibrations (A') give rise to polarized bands while the out-of-plane ones (A″) to depolarized band.

The detailed vibrational assignments of fundamental modes of 2A4P along with calculated IR, Raman intensities and normal mode descriptions (characterized by TED) were reported in Table 5. For visual comparison, the observed and simulated FT-IR and FT-Raman spectra of 2A4P are produced in a common frequency scales in Fig. 2 & Fig. 3.

Root mean square (RMS) values of frequencies were obtained in the study using the following expression,

$$RMS = \sqrt{\frac{1}{n-1}\sum_{i}^{n}\left(\upsilon_i^{calc} - \upsilon_i^{exp}\right)^2}$$

The RMS error of the observed and calculated frequencies (unscaled / B3LYP/6-311+G**) of 2A4P was found to be 106 cm^{-1}. This is quite obvious; since the frequencies calculated on the basis of quantum mechanical force fields usually differ appreciably from observed frequencies.

This is partly due to the neglect of anharmonicity and partly due to the approximate nature of the quantum mechanical methods. In order to reduce the overall deviation between the unscaled and observed fundamental frequencies, scale factors were applied in the normal coordinate analysis and the subsequent least square fit refinement algorithm resulted into a very close agreement between the observed fundamentals and the scaled frequencies. Refinement of the scaling factors applied in this study achieved a weighted mean deviation of 8.62 cm^{-1} between the experimental and scaled frequencies of the title compound.

Table 2. Optimized geometrical parameters of 2A4P obtained by B3LYP/ 6–311+G density functional calculations**

Bond length	Value(Å)	Bond angle	Value(Å)	Dihedral angle	Value(Å)
N2-C1	1.30140	C3-N2-C1	120.00100	C4-C3-N2-C1	0.00000
C3-N2	1.30136	C4-C3-N2	123.33033	C5-C4-C3-N2	0.00000
C4-C3	1.26127	C5-C4-C3	116.66866	N6-C1-N2-C3	0.00000
C5-C4	1.38600	N6-C1-N2	120.00100	N7-C1-N6-C5	-179.42809
N6-C1	1.30136	N7-C1-N6	119.99632	H8-C3-C4-C5	-179.45460
N7-C1	1.44599	H8-C3-C4	118.33274	H9-C4-C5-N6	-179.39400
H8-C3	1.12191	H9-C4-C5	121.66562	O10-C5-N6-C1	-179.42754
H9-C4	1.12198	O10-C5-N6	119.99801	H11-N7-C1-N6	0.00000
O10-C5	1.40997	H11-N7-C1	120.00391	H12-N7-C1-N6	-179.42718
H11-N7	1.02793	H12-N7-C1	119.99668	H13-O10-C5-N6	0.00391
H12-N7	1.02801	H13-O10-C5	109.50241		
H13-O10	0.99194				

*for numbering of atom refer Fig. 1

Table 3. Definition of internal coordinates of 2A4P

No(i)	Symbol	Type	Definition
Stretching			
1-7	r_i	C-N(aro)	C1-N2,C5-N6,C1-N7, N2-C3,N6-C1,N7-H12,N7-H11
8-9	S_i	C-C (sub)	C3-C4,C4-C5
10	s_i	C-O(sub)	C5-O10
11	P_i	O-H(ring)	O10-H13
12-13	p_i	C-H(sub)	C3-H8, C4-H9
Bending	α_i	C-N-C(ring)	C1-N2-C3,N2-C3-C4,C3-C4-C5,
14-19			C4-C5-N6,C5-N6-C1,N6-C1-N2
20-21	θ_i	N-C-H	N2-C3-H8, C4-C3-H8
22-23	β_i	C-C-H	C3-C4-H9, C5-C4-H9
24-25	Φ_i	C-C-O	C4-C5-O10, N6-C5-O10
26-27	γ_i	N-C-N	N6-C1-N7, N2-C1-N7
28-29	μ_i	C-N-H	C1-N7-H11, C1-N7-H12
30	ν_i	H-N-H	H11-N7-H12
31	φ_i	C-O-H	C5-O10-H13
Out-of-plane	ω_i	C-H	H8-C3-N2-C4,H9-C4-C3-C5
32-33			
34	ξ_i	C-O	O10-C5-C4-N6
35-36	λ_i	C-N	N7-C1-N6-N2, C1-N7-H11-H12
Torsion			C1-N2-C3-C4,N2-C3-C4-C5,
37-42	τ_i	τC-N	C3-C4-C5-N6,C4-C5-N6-C1, C5-N6-C1-N2,N6-C1-N2,C3
43	τ_i	τH-O	H13-O10-C5-C4(N6)
44	τ_i	τNH2	N6(N2)-C1-N7-H11(H12)

*for numbering of atom refer Fig. 1

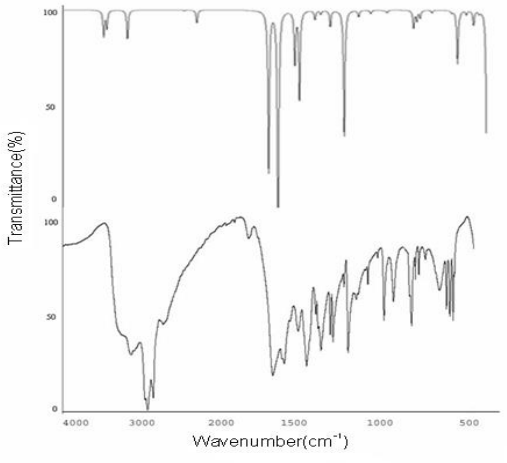

Fig. 2. FT-IR spectra of 2A4P
(a)Observed (b) Calculated with B3LYP/6-311+G**

Table 4. Definiton of local symmetry coordinates and the value corresponding scale factors used to correct the force fields for 2A4P

No.(i)	Symbol[a]	Definition[b]	Scale factors used in calculation
1-7	C-N(aro)	r1,r2,r3,r4,r5,r6,r7	0.914
8-9	C-C(sub)	S8,S9	0.914
10	C-O(sub)	s10	0.992
11	O-H(ring)	P11	0.992
12-13	C-H(sub)	p12, p13	0.916
14	C-N-C(ring)	(α14-α15+α16-α17+α18-α19)/ √6	0.992
15	C-N-C(ring)	(2α14-α15-α16+2α17-α18-α19)/ √12	0.992
16	C-N-C(ring)	(α15-α16+α18-α19)/2	0.992
17	N-C-H	(θ20-θ21)/√2	0.923
18	C-C-H	(β22-β23)/√2	0.923
19	C-C-O	(Φ24-Φ25)/√2	0.991
20	N-C-N	(γ26-γ27)/√2	0.967
21	C-N-H	(μ28-μ29)/√2	0.923
22	H-N-H	ν30	0.918
23	C-O-H	Φ31	0.962
24-25	C-H	ω32, ω33	0.994
26	C-O	ξ34	0.962
27-28	C-N	λ35, λ36	0.961
29	tring	(τ37-τ38+τ39-τ40+τ41-τ42)/√6	0.994
30	tring	(τ37-τ39+τ40-τ42)/2	0.994
31	tring	(-τ37+2τ38-τ39-τ40+2τ41-τ42)/√12	0.994
32	H-O	τ43/2	0.979
33	NH2	τ44/4	0.896

a These symbols are used for description of the normal modes by TED in Table 5.
b The internal coordinates used here are defined in Table 3.

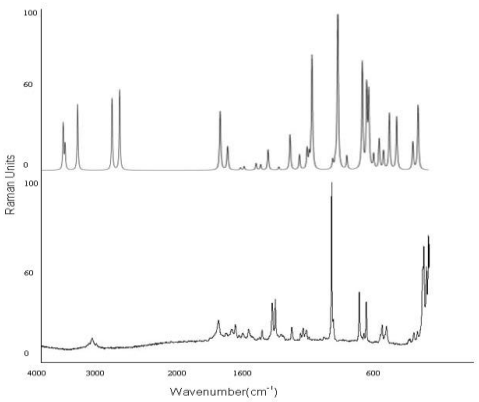

Fig. 3. FT-Raman spectra of 2A4P
(a) Observed (b) Calculated with B3LYP/6-311+G**

C–H vibrations

Aromatic compounds commonly exhibit multiple weak bands in the region 3100–3000 cm^{-1} due to aromatic C–H stretching vibrations. Accordingly, in the present study the C–H vibrations of the title compounds are observed at 3131, 2956, 2925, 2864 cm^{-1} in the FTIR spectrum and 3010 cm^{-1} in Raman for 2A4P. The bands due to C–H in-plane ring bending vibration interacting some what with C–C stretching vibration are observed as a number of m-w intensity sharp bands in the region 1300–1000 cm^{-1}. C–H out-of-plane bending vibrations are strongly coupled vibrations and occur in the region 900–667 cm^{-1} [10]. The in-plane and out-of-plane bending vibrations of C–H have also been identified for the title compound.

O-H vibrations

The precise positions of O–H band are dependent on the strength of hydrogen bond. The O–H stretching appears at 3300–3000cm^{-1} in the inter-molecular hydrogen bonded systems. The title compound in this study showed a very strong absorption peak at 3724 cm^{-1} which are due to the O–H stretching vibrations. The observed peaks in this region are sharp and strong. The in-plane and out-of-plane bending vibration of the hydroxyl groups are identified.

C–O vibrations

If a compound contains a carbonyl group, the absorption caused by the C–O stretching is generally strongest [11]. Considerations of these factors lead to assign the band observed at 1407 cm^{-1} to C–O stretching vibrations for the title compound.

C–C vibration

The highest C–C stretching vibration of benzene is around 1600 cm^{-1}. In substituted benzene, the vibrations should appear near 1600 cm^{-1} giving rise to a fairly strong bands IR and Raman spectra. In present investigation, the C-C mode mixes with C–H in-plane bending vibrations. The IR and Raman bands observed at 1519 cm^{-1} and 1501 cm^{-1}, respectively.

Amino group vibrations

The frequencies of amino group appear in the regions 3500–3300 cm^{-1} for N-H stretching, 1700–1600 cm^{-1} for scissoring and 1150–900 cm^{-1} for rocking deformations [12]. In the present study, the asymmetric and symmetric modes of NH_2 group were assigned at 3584 and 3706 cm^{-1}, respectively. The band observed at 1680 cm^{-1} in IR spectrum with PED contribution 28% is assigned to NH_2 scissoring mode. The rocking, wagging deformation vibrations of NH_2 contribute to several normal modes in the low frequency region. The band observed at 1079 cm^{-1} with PED contribution 26% is assigned to NH_2 rocking vibration and the band observed at 474 cm^{-1} with PED contribution 68% is assigned to NH2 wagging mode. The wagging and torsional modes of NH_2 were identified at 397 and 516 cm^{-1} with PED contribution of 23% and 9% respectively. They were also supported by the literature [13].

C-N vibrations

The identification of C-N vibrations is a difficult task, since the mixing of vibrations is possible in this region. However, with the help of force field calculations, the C-N vibrations are identified and assigned in this study. For the title compound it is observed at 1233 cm^{-1}. The slight shift in wavenumber in due to the fact that force constants of the C-N bond increases due to resonance with the ring [14]. Pyrimidinol absorb strongly in the region 1600–1500 cm^{-1} due to the C=C and C=N ring stretching vibrations [15]. Absorbances are also observed at 1640–1620 cm^{-1}, 1580–1520 cm^{-1}, 1000–960 cm^{-1} and 825–775 cm^{-1}. Accordingly the bands observed at 1678, 1519, 1498 and 984 cm^{-1} have been assigned to C-N stretching modes and their corresponding TED modes are, respectively.

Table 5. Detailed assignments of fundamental vibrations of 2A4P by normal mode analysis based on SQM force field calculation

S. No.	Symmetry species C_s	Observed frequency (cm^{-1})		Calculated frequency (cm^{-1}) with B3LYP/6-311+G ** force field				TED (%) among type of internal coordinates[c]
		Infrared	Raman	Unscaled	Scaled	IR[a] A_i	Raman[b] I_i	
1	A'			3730	3724	56.863	116.143	OH(100)
2	A'			3715	3706	38.762	60.974	CN(100)
3	A'	3500		3590	3584	63.263	144.235	CN(100)
4	A'		3200	3258	3250	1.553	114.126	CH(99)
5	A'	3131		3183	3176	27.765	118.730	CH(99)
6	A'	1678		1689	1681	354.759	19.291	CN(42),CC(22),bOH(10),bCO(9),bring(9),bCNH(7)
7	A'			1634	1626	245.476	2.949	bHNH(61),CN(30)
8	A'	1619	1624	1628	1622	287.261	5.261	CC(35),CN(28),bring(10),bCNH(10),bCH(8)
9	A'	1519		1530	1525	111.688	0.710	CN(30),bCH(22),bCNH(21),CO(12)
10	A'		1501	1510	1498	188.243	1.082	CN(53),bHNH(21),bring(10),bCNH(9)
11	A'	1409		1416	1407	19.452	1.668	CN(32),CO(19),bring(15),bCH(13),bOH(9),CC(7)
12	A'	1377		1380	1373	8.414	1.287	CN(34),bCNH(33),bNH(9),bOH(8),bCN(7)
13	A'	1318		1323	1316	32.756	4.423	CN(59),CC(18),CO(7),bOH(7)
14	A'	1233	1232	1240	1234	278.490	0.647	CN(36),bOH(32),CO(16),CC(12)
15	A'			1157	1150	15.155	6.123	bCH(40),CC(28),bNH(18)
16	A'	1082	1089	1085	1078	7.851	2.371	bNH(25),CN(23),CC(16),bOH(8),CO(7),bCO(7)
17	A"		1025	1029	1019	0.427	2.990	gCH(92),tring(7)
18	A'	1021	1007	1011	1005	1.554	1.696	CN(28),bring(24),bNH(24),CC(17)
19	A'	982		990	984	5.955	15.963	CN(52),bring(35)
20	A"	821		835	824	33.883	0.952	gCH(73),gCO(14),tring(13)
21	A"		797	815	810	28.309	0.458	tring(53),gCN(33),gCO(7),gCH(6)
22	A'	786		796	788	17.031	16.507	bring(42),CN(18),CC(17),CO(13)
23	A"	722		725	721	1.465	1.045	gCO(49),tring(24),gCN(23)
24	A'			608	602	6.190	7.056	bring(76),CN(15)
25	A"		562	574	569	120.340	4.997	tHO(84),tring(10)
26	A'	550	545	559	553	4.945	4.404	bring(74),CO(8),bCO(6),CN(5)
27	A'			523	516	14.782	0.556	bCO(39),bCN(26),bring(12)
28	A"			480	462	10.002	0.169	tring(50),gCN(14),gCH(14),gCO(11)
29	A"		429	448	434	43.065	2.225	tNH2(64),tring(11),gCN(7)
30	A"			405	397	306.920	2.052	gCN(62),bHNH(23),CN(9)
31	A'		397	330	343	4.106	1.509	bCN(48),bCO(16),bNH(11),bring(9),tNH2(8),CN(6)
32	A"			236	228	2.805	0.425	tring(76),gCH(9),gCO(8),gCN(7)
33	A"		197	205	190	3.786	0.632	tring(87),gCH(11)

Abbreviations used: b, bending; g, wagging; t, torsion; s, strong; vs, very strong; w, weak; vw, very weak;

[a] Relative absorption intensities normalized with highest peak absorption

[b] Relative Raman intensities calculated by Eq.1 and normalized to 100.

[c] For the notations used see Table 4.

Hyperpolarizability calculations

The first-order hyperpolarizibility (β_{ijk}) of the novel molecular system of PNBC is calculated using 3-21 G (d,p) basis set based on finite field approach. Hyperpolarizibility is a third rank tensor that can be described by a 3 x 3 x 3 matrix. It strongly depends on the method and basis set used. The 27 components of 3D matrix can be reduced to 10 components due to Kleinman [16] symmetry. The calculated first-order hyperpolarizability (β_{total}) of 2A4P is $1.28432x10^{-30}$ esu, which is nearly 7 times greater than that of urea (0.1947×10^{-30} esu). The calculated dipole moment (μ) and first-order hyperpolarizibility (β) are shown in Table 6. The theoretical calculation seems to be more helpful in determination of particular components of β tensor than in establishing the real values of β. Domination of particular components indicates on a substantial delocalization of charges in those directions. It is noticed that in β_{zxx} (which is the principal dipole moment axis and it is parallel to the charge transfer axis) direction, the biggest values of hyperpolarizability are noticed and subsequently delocalization of electron cloud is more in that direction. The higher dipole moment values are associated, in general, with even larger projection of β_{total} quantities. The electric dipoles may enhance, oppose or at least bring the dipoles out of the required net alignment necessary for NLO properties such as β_{total} values. The connection between the electric dipole moments of an organic molecule having donor–acceptor substituent and first hyperpolarizability is widely recognized in the literature [17]. The maximum β was due to the behavior of non-zero μ value. One of the conclusions obtained from this work is that non-zero μ value may enable the finding of a non-zero β value. Of course Hartee–Fock calculations depend on the mathematical method and basis set used for a polyatomic molecule.

Table 6. The dipole moment (μ) and first-order hyperpolarizibility (β) of 2A4P derived from DFT calculations

β_{xxx}	0.578808
β_{xxy}	0.0089869
β_{xyy}	0.0200478
β_{yyy}	-0.00104341
β_{zxx}	1.20816
β_{xyz}	0.00601775
β_{zyy}	0.00230936
β_{xzz}	0.321359
β_{yzz}	0.00580402
β_{zzz}	-0.314651
β_{total}	1.28432
μ_x	0.031339267
μ_y	0.0000787639
μ_z	0.166331345
μ	0.444690202

Dipole moment (μ) in Debye, hyperpolarizibility $\beta(-2\omega;\omega,\omega)$ 10^{-30}esu.

Conclusions

IR and Raman Spectra were obtained for 2A4P, in which all of the expected 33 normal modes of vibration were assigned. The optimized molecular geometry, force constants and vibrational frequencies were calculated using DFT techniques in the B3LYP approximation.

Taking the observed frequencies as a basis corresponding to the fundamental vibrations, it was possible to proceed to a scaling of the theoretical force field.

The resulting SQM force field served to calculate the potential energy distribution, which revealed the physical nature of the molecular vibrations, and the force constants in internal coordinates, which were similar to the values obtained before for related chemical species. The first-order hyperpolarizibility (β_{ijk}) of the novel molecular system of 2A4P is calculated using 3-21 G (d,p) basis set based on finite field approach. The calculated first-order hyperpolarizability (β_{total}) of 2A4P is $1.28432x10^{-30}$ esu, which is nearly 7 times greater than that of urea (0.1947×10^{-30} esu).

References

[1] A.D. Becke, J. Chem. Phys., 98 (1993) 5648.
[2] C. Lee, W. Yang, R.G. Parr, Phys. Rev., B37 (1988) 785.
[3] A. Frisch, A.B. Nielson and A.J. Holder, Gaussview Users Mannual, Gaussian Inc., Pittsburgh, PA (2000).
[4] T. Sundius. J.Mol. Struct., 218 (1990) 321.
[5] P.L. Polavarapu, J. Phys. Chem. 94, 8106 (1990).
[6] G. Keresztury, S. Holly, J. Varga, G. Besenyei, A.V. Wang, J.R. Durig, Spectrochim. Acta 49A,2007 (1993).
[7] G. Keresztury, in: J.M. Chalmers and P.R. Griffiths(Eds), Handbook of Vibrational Spectroscopy vol.1, John Wiley & Sons Ltd. p. 71, (2002).
[8] H.D. Cohen, C.C.J. Roothan, J. Chem. Phys. S34, 435 (1965).
[9] P. Pulaaay, G. Fogarasi, G.Pongor, J. E. Boggs, A. Vargha, J. Am. Chem. Soc., 105 (1983) 7037.
[10] J. Mohan, Organic Spectroscopy-Principles and Applications, second ed., Narosa Publishing House, New Delhi, 2001.
[11] W.D. Bowman, T.G. Spiro, J. Bhem. Phys. 73 (1980) 5482.
[12] G. Socrates, Infrared and Raman Characteristic Group Frequencies, Tables and Charts, third ed., Wiley, Chichester, 2001.
[13] Z. Niu, K.M. Dunn, J.E. Boggs, Mol. Phys. 55 (1985) 421.
[14] G. Varsanyi, Vibrational Spectra of Benzene Derivatives, Academic Press, New York, 1961.
[15] B.K. Sharma, Spectroscopy, 11th ed., GOEL Publishing House, Meerut,1995/1996.
[16] D.A. Kleinman, Phys. Rev. 1962;126,1977.
[17] P.N. Prasad, D.J. Williams, Introduction to Nonlinear Optical Effects in Molecules and Polymers, Wiley, New York, (1991).